Spectral Non-Stationarity in Road Vehicle Vibrations

László Róbert Hári[1*]

[1] Department of Logistics and Forwarding, Audi Hungaria Faculty of Automotive Engineering, Széchenyi István University, Egyetem tér 1., H-9026 Győr, Hungary
[*] Corresponding author, e-mail: hari.laszlo@sze.hu

Abstract

Road-induced vibrations are in the scope of various environmental testing protocols, e.g., for packaging vibration testing (PVT) purposes. This field matures with well-understood methods for analyzing amplitude-type non-stationarity (NS) in road vehicle vibrations (RVV). Albeit frequency-type NS is well known, only suggestions are provided for processing the phenomenon in PVT. Both types of NS can be jointly investigated in the time-frequency domain; thus, the current study initiates the investigation of spectral non-stationarities (SNS) in RVV. Three vibration series were recorded from 118 km traveled distance supplying an empirical insight.

Keywords

changepoint-detection, reverse arrangements test, road vehicle vibration, spectral moments, spectral non-stationarity

1 Introduction

Statistics, econometrics, and acoustics are typically concerned with the challenge of time series' stationarity. It may be impractical to indulge in a comprehensive listing; instead, the current paper discusses the results in the context of packaging vibration testing (PVT). The discipline of PVT is fundamentally involved with non-stationarity (NS), present in road vehicle vibrations (RVV). Scholars have presented various methods accounting for amplitude-type NS. Albeit the phenomenon of frequency-type or spectral non-stationarities (SNS) is pointed out, mostly suggestions are provided. Therefore, the current article presents an empirical validation of the presence of SNS in RVV obtained by three measurements in a passenger car, such as:

$$H_0 : \text{ SNS does not exist in RVV,} \qquad (1)$$

$$H_A : \text{ SNS exist in RVV.}$$

It is assumed under H_0 that spectral moments of the measured RVV are stationary over time. The reverse arrangements test (RA) is used to assess the null hypothesis, and the study is augmented by changepoint analysis (CPA).

A stochastic process is said to be stationary in the strong sense if its unconditional joint probability distribution does not change when shifted in time (Gagniuc, 2017). On the other hand, the exact process is said to be stationary in the wide sense if its mean and auto-covariance do not vary with respect to time. Simply put, if the mean and autocorrelation

function of a stochastic process is time-invariant, the process is weakly stationary; and the process is strictly stationary if all moments are time-independent (Faber, 2012:p.74).

Parametric models, frequently used for stationarity testing, cover the augmented Dickey and Fuller (1981) test for a unit root, the KPSS test (Kwiatkowski et al., 1992), the Leybourne and HcCabe (1999) stationarity test, and the Phillips and Perron (1988) test for one unit root. The above tests, however, rely on model assumptions in the form of autoregressive integrated moving average (ARIMA) processes. Therefore, one might turn toward alternative solutions without a specific model in question. A semi-parametric analysis is the variance ratio test (VR) for a random walk, initially suggested by Lo and MacKinlay (1988). The VR investigates the random walk hypothesis against stationary alternatives (Pradhan, 2012).

Non-parametric methods, also devoted to stationarity problems, include the runs test (David and Siegel, 1957:p.538), the reverse arrangements test (RA) (Bendat and Piersol, 2010:p.97), and the modified RA test (Bilodeau et al., 1997). Unfortunately, the three non-parametric tests can show inconsistencies, as discussed later.

The current study suggests the changepoint detection in spectral descriptors from the time-frequency domain of recordings to strengthen the investigation of stationarity. Control charts introduced by Shewhart and Deming (1986) are typical examples in manufacturing to monitor and

control *capable* processes. Statistical process control (SPC) can be enhanced by CPA. While SPC can be updated at each incoming sample, CPA can be performed once all data points are collected. SPC detects abnormal observations and major changes, but CPA can also find minor changes and controls the change-wise error rate (Taylor, 2000).

The establishment of CPA can be credited to Page (1954; 1955; 1957), who developed a test for a change in a parameter occurring at an unknown point. The setup of the problem consists of independent observations x_n for $n = 1, ..., N$ ordered in time, incurring a changepoint at $n = m$. The procedure investigates whether all the observations are from the same population with the distribution function $F(x|\Theta)$, i.e., under the alternative $x_{n = 1, ..., m}$ are from $F(x|\Theta)$ and $x_{n = m + 1, ..., N}$ come from $F(x|\Theta')$ $(\Theta = \Theta')$. The cumulative sum (CUSUM) schemes are further discussed in Subsection 2.5, which are commonly sharpened by resampling methods. In short, the probability of the changepoint's actual existence can be assessed by a corresponding *p*-value from a resampling technique.

2 Materials and methods
Section 2 presents first the details of experiments and the pre-processing of the recorded vibration series. It is accompanied by introducing the considered spectral descriptors, the RA test, and the CPA, the latter including a permutation resampling method assessing the significance of candidate changepoints.

2.1 Experimental
Three measurements are recorded on routes A, B, and C, reported in Fig. 1. Capitals denote the experiments, and lower-case letters signify sub-figures throughout the paper. Common factors are the passenger car (Suzuki Swift Sedan 1.3 GLX year 2002), the personnel (one chauffeur and one experimentist, approx. 150 kg in total), the GPS position recorder (Columbus P1, $f_s^{(gps)} = 1$ Hz), the DC MEMS accelerometer (Recovib Tiny 15G, $f_s^{(acc)} = 1024$ Hz, effective bandwidth 250 Hz). The accelerometer's placements are:

1. in the coin toss attached with thick double-sided tape,
2. on the right-hand side upper plane of the cockpit attached with thin double-sided tape, and
3. in the trunk on the right-hand side attached to the chassis with magnets.

The traveled distances are:
1. 35.50,
2. 29.88, and
3. 52.53 km, respectively.

2.2 Preprocessing
The current method relies on the short-time Fourier transform (STFT) with one-sec non-overlapping Boxcar windows yielding an equidistant 1 Hz and 1 sec resolution. The power spectral densities (PSD) in Fig. 1. *d)* are given up to the Nyquist frequencies. In other cases, STFT spectrograms are band-limited to [1, 250] Hz with an ideal numerical band-pass filter. Fig. 2 depicts only [1, 175] Hz intervals for further readability.

2.3 Spectral moments
The RA test and CPA are applied to the first four spectral moments denoted by μ_i for $i = 1, 2, 3, 4$, respectively, the spectral centroid, ~ spread, ~ skewness, and ~ kurtosis. The frequency-weighted sum of s_k spectral values normalized by the unweighted sum is the spectral centroid (The MathWorks, Inc., 2021):

$$\mu_1 = \frac{\sum_{k=b_1}^{b_2} f_k s_k}{\sum_{k=b_1}^{b_2} s_k}, \tag{2}$$

where f_k is the k-th frequency bin in Hz. The bandwidth is given by b_1 and b_2 bins. The spectral centroid can be used in music interpretation and genre identification as a brightness measure (Grey and Gordon, 1978). The spectral spread is defined as the standard deviation across the spectral centroid, which stands for the spectrum's instantaneous bandwidth (The MathWorks, Inc., 2021):

$$\mu_2 = \sqrt{\frac{\sum_{k=b_1}^{b_2} (f_k - \mu_1)^2 s_k}{\sum_{k=b_1}^{b_2} s_k}}. \tag{3}$$

The spread, for instance, widens as the tones diverge and narrows as they converge. Spectral skewness is a metric that calculates symmetry around the centroid (The MathWorks, Inc., 2021):

$$\mu_3 = \frac{\sum_{k=b_1}^{b_2} (f_k - \mu_1)^3 s_k}{(\mu_2)^3 \sum_{k=b_1}^{b_2} s_k}. \tag{4}$$

Spectral skewness can discern the articulation point (Jongman et al., 2000), showing the relative frequency of higher and lower harmonics in harmonic signals. The spectral kurtosis is a measure of the spectrum's flatness (or non-Gaussianity) around the centroid (The MathWorks, Inc., 2021):

$$\mu_4 = \frac{\sum_{k=b_1}^{b_2} (f_k - \mu_1)^4 s_k}{(\mu_2)^4 \sum_{k=b_1}^{b_2} s_k}, \tag{5}$$
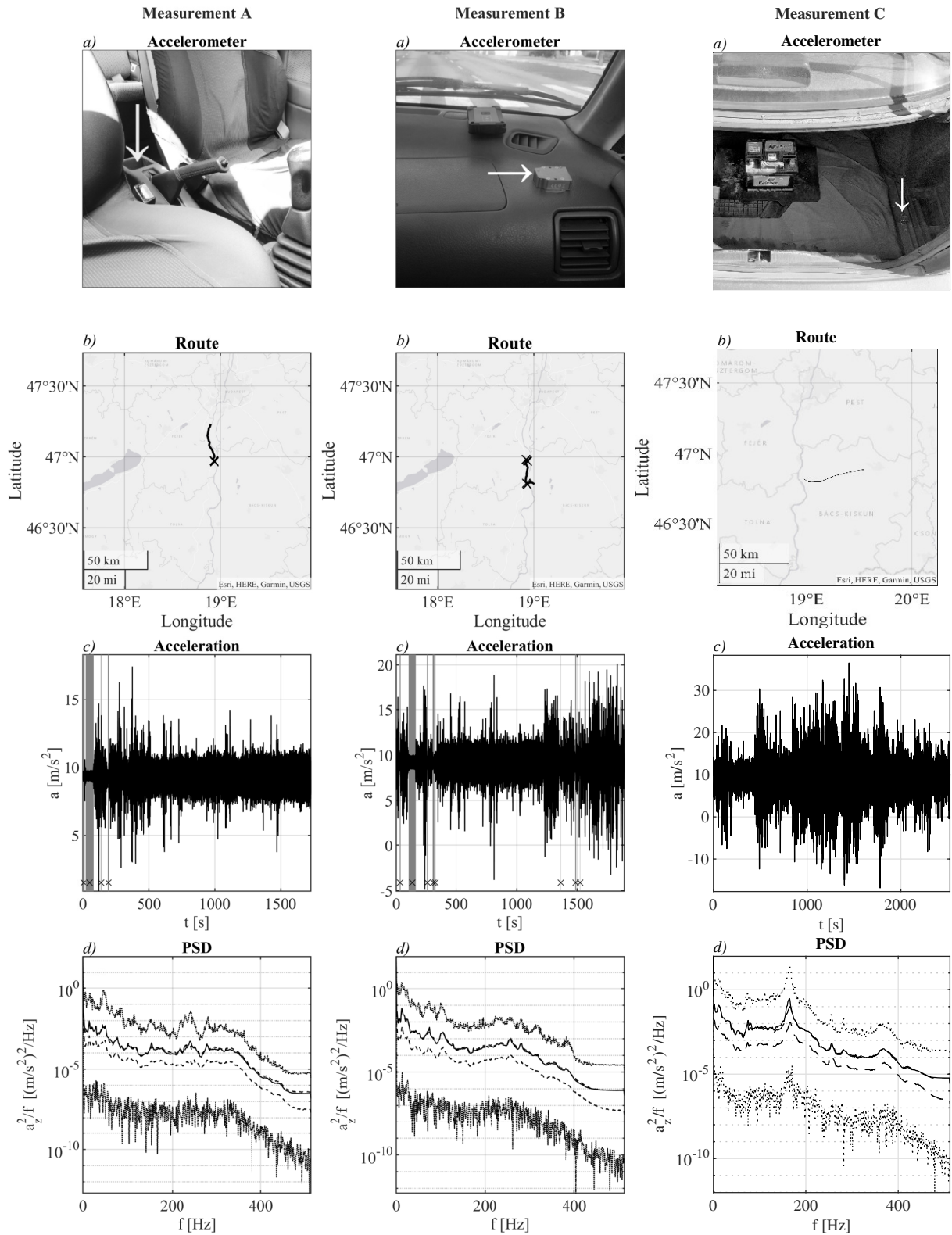
Fig. 1 A, B, C measurements per column. Each measurement is accompanied by rows of *a)* place of accelerometer, *b)* GPS coordinates, stops marked by *crosses* (✕), *c)* vertical acceleration with the notion of stops (✕ *on grey intervals*), and *d)* power spectral density. In panes *d)* the average (*solid*), 25th and 75th percentiles (*dashed*), and the max-min envelopes over time (*dotted*) are plotted. Note that the 75th percentile is likely to overlap with the average
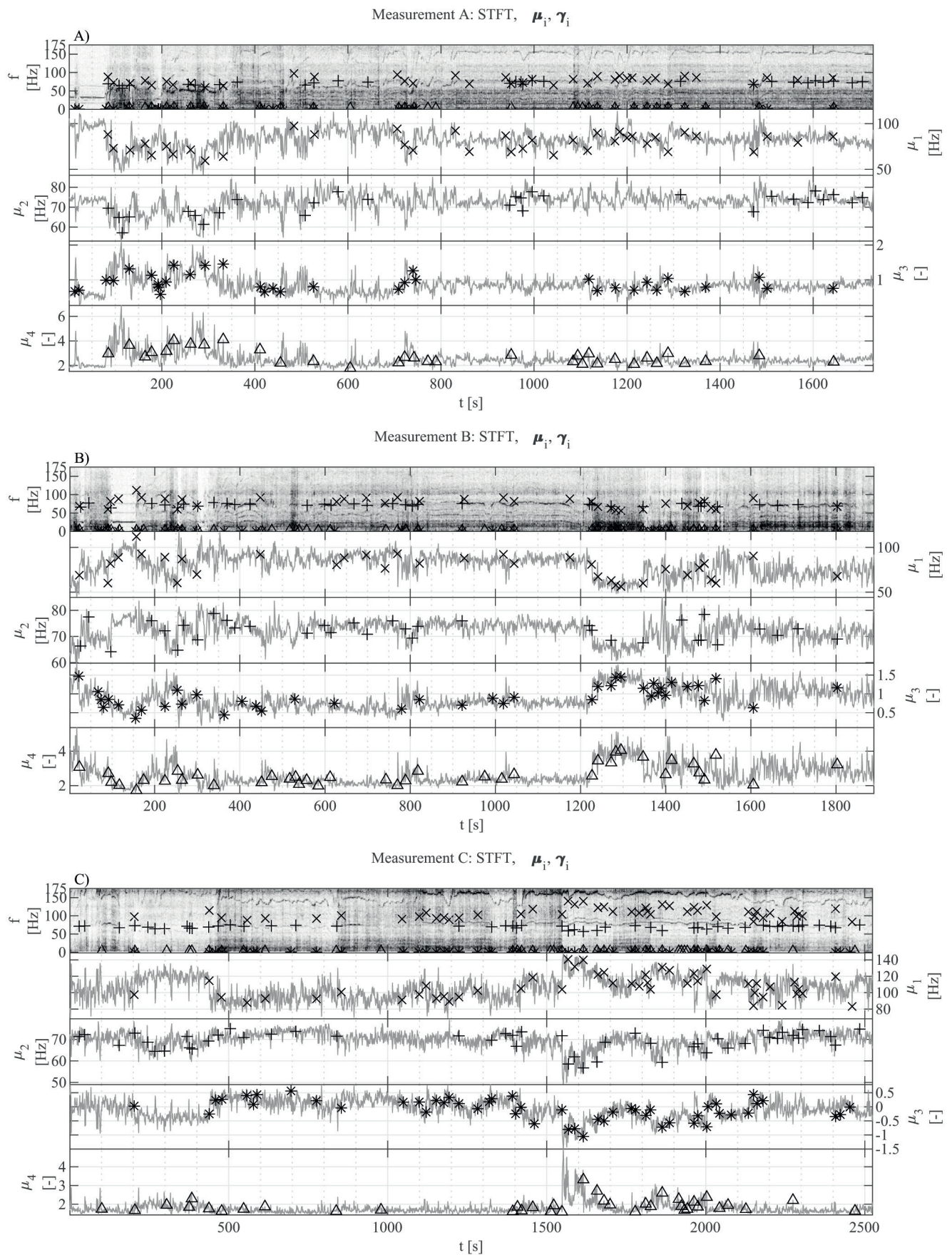
Fig. 2 Short-time Fourier (STFT) transforms of measurements A, B, C. Below each STFT, spectral moments μ_i for $i = 1, 2, 3, 4$ corresponding to the spectral centroid, ~ spread, ~ skewness, and ~ kurtosis are plotted. The first panes also show the changepoints by different symbols

showing the peaked nature of a spectrum. Therefore, an increasing white noise on tonal components yields a decreasing kurtosis indicating a spectrum with less peaky character. The Discussion introduces other frequency domain measures like entropy, flatness, crest, flux, slope, decrease, and roll-off point.

2.4 Reverse arrangements test

The RA test (Bendat and Piersol, 2010:p.97) is a non-parametric test that does not assume any underlying distribution, trend, or model. It evaluates a sequence of ordered data obtained from independent observations of the same random variable by deciding if the observations undergo a significant trend. The n-th reverse arrangement A_n is the number of times that $x_n > x_m$ for $n < m$ given a sequence of N observed values of a random variable, x_n for $n = 1, ..., N$. Then A_n is summed to get the total number of reverse arrangements, $A = \sum_{n=1}^{N-1} A_n$. Given x_n is a collection of N independent observations of the same random variable, A is a random variable with the mean of:

$$\mu_A = N\left(\frac{N-1}{4}\right), \tag{6}$$

and variance:

$$\sigma_A^2 = N(N-1)\left(\frac{2N+5}{72}\right). \tag{7}$$

Then, A is expected to be above or below of μ_A when an increasing or a decreasing trend underlies the data. Albeit tabulated values of A are available, the tendency to normality is highly rapid for $N \geq 14$ and:

$$z = \frac{A - \mu_A}{\sigma_A}, \tag{8}$$

approximately follows the standard normal distribution. The z-value is used to reject H_0, thus Eq. (1) can be written as:

$$H_0 : \mu_A = 0, \tag{9}$$

$$H_A : \mu_A \neq 0.$$

2.5 Changepoint detection

The method is individually set up in Matlab based on the work presented by Taylor (2000). The CPA is applied here on $x = x_n = \mu_i$, such as:

$$S_n = \sum_{n=1}^{N} (x_n - \bar{\bar{x}}), \tag{10}$$

where:

$$\bar{\bar{x}} = \frac{1}{N} \sum_{n=1}^{N} x_n,$$

that is the cumulative sum of differences between x_n and its total mean, $\bar{\bar{x}}$, is computed. The extremum $\hat{S}_n$ yields a candidate changepoint at $\mu_{i,m}$ and the permutation loop decides upon the significance. Each reference set comprises $R = 10^4$ permutations, and an $\alpha = 0.05$ significance limit is chosen for demarcation. The interested reader is referred to Kowalewski and Novack-Gottshall (2010) for a comprehensive overview of resampling methods. A difference compared to Taylor (2000) emanates from using the same S_n statistic Eq. (10) at each permutation, instead of $\max S_n - \min S_n$. Given a significant changepoint at μ_{i,m^*}, the i-th series μ_i is divided into two parts: $n = 1, ..., m^*$ and $m^* + 1, ..., N$, each submitted to the same CPA until no more changepoint is found. The programmatic realization of the algorithm will be published in Hári and Földesi (2022).

The cardinality of significant changepoints per the i-th spectral moment is symbolized by $\gamma_i = \#\{m^*\}$. The number of unique and significant changepoints for the set of μ_i is:

$$\Gamma = \#\left\{\bigcup_{i=1}^{4} \gamma_i\right\}. \tag{11}$$

Finally, the temporal density of changepoints is proposed:

$$°\Gamma = \Gamma / T, \tag{12}$$

where T is the length of the recording. The following reporting scheme is recommended for RVV analysis accommodating the method in large-scale experiments and cross-validation studies:

$$°\Gamma = °\Gamma(\mu_i, R, \alpha, \Delta t, \Delta f)[1/s], \tag{13}$$

with Δt, Δf time- and frequency resolution of the DFT-based spectrogram, respectively.

3 Results

The results supported the investigated alternative hypothesis in Eq. (1). The spectral moments $\mu_i^{(j)}$ for $i = 1, 2, 3, 4$ in $j = A, B, C$ show at least $\text{cv}(\mu_2^{(C)}) = 5.41\%$ and at most $\text{cv}(\mu_3^{(C)}) = -461.32\%$ coefficient of variation. The null hypothesis of stationarity Eq. (9) is rejected in favor of the *alternative* by the RA test at the $\alpha = 0.05$ significance level in all cases, but $\mu_1^{(A)}$, $\mu_3^{(A)}$, and $\mu_4^{(C)}$. Therefore, measurements A, B, and C can undergo spectral non-stationarity since at least one of four spectral moments per experiment is non-stationary. It is worth recalling that SNS is present regardless of the accelerometer's fixture and position.

While RA tests confirmed SNS in most cases, the CPA delivers further insights into the non-stationarity since no changepoints would be expected under H_0. First, let us not consider the spatial- or temporal distribution of changepoints in Fig. 2. Then, 2.65, 3.35, 2.46 [1/km] unique changepoints per kilometer for routes A, B, and C show that roughly each traveled kilometer incurred two to three different spectral characteristics, on average.

Here, $°\Gamma^{(A)} = 5.44 \cdot 10^{-2}$, $°\Gamma^{(B)} = 5.29 \cdot 10^{-2}$, and $°\Gamma^{(C)} = 5.11 \cdot 10^{-2}$ [1/sec] for ($\{\mu_1, \mu_2, \mu_3, \mu_4\}$, 104, 0.05, 1 sec, 1 Hz) are found.

Changepoints' temporal density is lower than spatial density [1/km]. Still, vibration testing protocols are also extended, e.g., "*the exposure duration for common carrier/truck is 60 minutes per 1609 kilometers (...) of road travel (per axis)*" (US Army Test and Evaluation Command, 2019, p.514.8C-16). Results from Table 1. signified by (*), imply that the RA test did not yield test statistics extreme enough to reject H_0. However, CPA found several changepoints considered significant. The three instances (*) are further discussed in Section 4.

4 Discussion

In principle, one could choose only the spectral mean for changepoint analysis since $\mu_2 = f(\mu_1)$, $\mu_3 = g(\mu_1)$, and $\mu_4 = h(\mu_1)$. However, it is interesting that a change in μ_1 does not imply changes in other descriptors and vice versa. Albeit the necessary number of spectral descriptors remains out of the scope, it is recommended to consider higher-order moments simultaneously.

Slight inconsistencies are pointed out by (*) between the RA test and the CPA, namely, changepoints have been found in series deemed stationary in the RA test. Beck et al. (2006) showed that the runs test, RA test, and modified RA test showed false negative and false positive results and deduced that these tests are not always reliable for stationarity testing. The hypothesized reason was that the above three trials had been primarily designed for checking randomness under H_0 or deciding the existence of an underlying trend under H_A. Therefore, it is also possible in the current experiment, that results marked by (*) are false negatives since changepoints are present. Furthermore, the autocorrelation of the

Table 1 Statistics of the spectral moments and their coefficients of variation, reverse arrangements tests, changepoints, unique changepoints, and temporal density of changepoints of measurements A, B, C

	Statistics	A	B	C
(a)	$\bar{\mu}_1 \pm \sigma(\mu_1)$	83.06 ± 10.36	80.52 ± 12.30	105.77 ± 14.11
	$\bar{\mu}_2 \pm \sigma(\mu_2)$	72.68 ± 4.62	72.31 ± 3.94	69.82 ± 3.77
	$\bar{\mu}_3 \pm \sigma(\mu_3)$	0.85 ± 0.24	0.87 ± 0.28	−0.07 ± 0.34
	$\bar{\mu}_4 \pm \sigma(\mu_4)$	2.51 ± 0.62	2.63 ± 0.62	1.79 ± 0.31
(b)	cv_1	12.47	15.28	13.34
	cv_2	6.36	5.45	5.41
	cv_3	28.86	32.24	−461.32
	cv_4	24.77	23.44	17.63
(c)	z_1 (p) [H]	(*) 0.17 (0.87) [0]	16.85 (0.00) [1]	−10.67 (0.00) [1]
	z_2 (p) [H]	−11.37 (0.00) [1]	7.59 (0.00) [1]	3.75 (0.00) [1]
	z_3 (p) [H]	(*) 1.91 (0.06) [0]	−17.21 (0.00) [1]	9.45 (0.00) [1]
	z_4 (p) [H]	3.20 (0.00) [1]	−15.16 (0.00) [1]	(*) −1.14 (0.25) [0]
(d)	γ_1	38	35	49
	γ_2	29	35	49
	γ_3	35	42	51
	γ_4	33	41	38
(e)	Γ	94	100	129
(f)	$°\Gamma$	$5.44 \cdot 10^{-2}$	$5.29 \cdot 10^{-2}$	$5.11 \cdot 10^{-2}$

(a) mean ± standard deviation [m/s²];
(b) coefficient of variation $cv_i [\%] = 100 \cdot \sigma(\mu_i) / \bar{\mu}_i$;
(c) z-value (two tails significance) [= 1 if H_A; = 0 if H_0 at α = 0.05];
(d) significant changepoints at α = 0.05;
(e) number of unique changepoints in $\{\mu_1, \mu_2, \mu_3, \mu_4\}$;
(f) temporal density of changepoints [1/s];
(*) non-significant RA tests are further discussed in Fig. 3.

corresponding spectral moments shows variation with respect to time, as presented in Fig. 3.

Rouillard (2014) presented his approach by using runs tests on the moving RMS series from RVV measurements, which can detect only amplitude-type NS. However, the window width should be justified if one wishes to use moving statistics. In contrast, the current method analyzed the time-frequency domain of measurements, which can address amplitude- and frequency-type NS at the same time. Id. presented his solution based on the runs
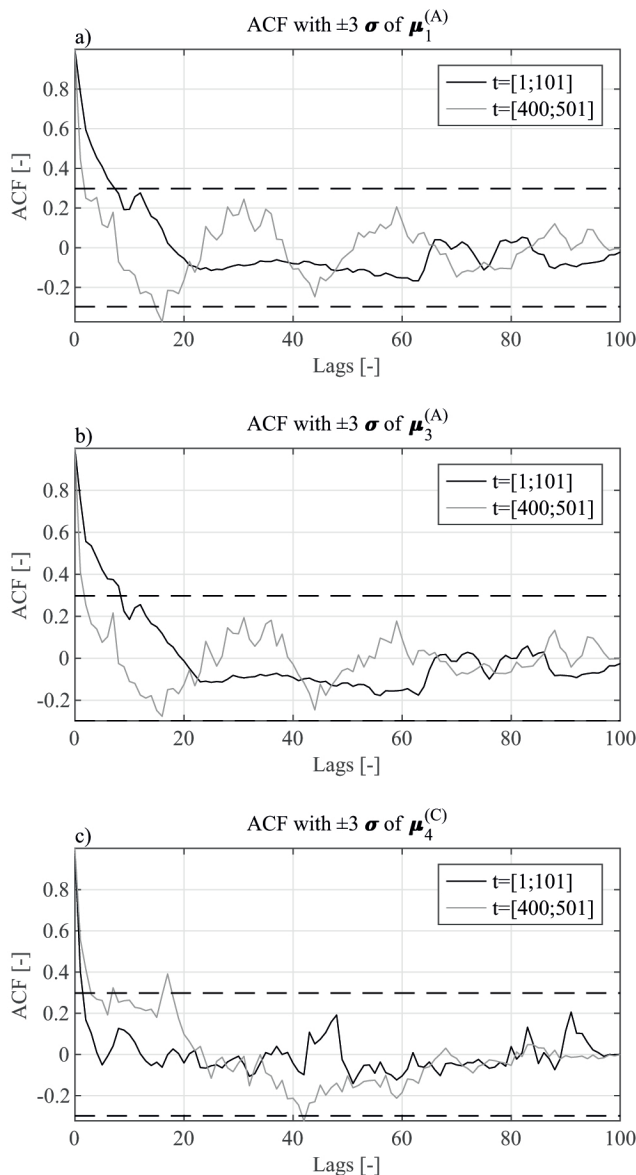
Fig. 3 Examples of changing autocorrelation function (ACF) (*solid*) showing confidence intervals estimated by ± three standard deviations (*dashed*): *a)* spectral centroid of short-time Fourier transform (STFT) from measurement A; *b)* spectral skewness of STFT from measurement A; and *c)* spectral kurtosis for measurement C. Note, how ACF changes at different intervals.

test. Stationary Gaussian vibrations were also subjected to the runs test as falsification trials, which produced true negative results in three of four cases of different moving RMS time histories of stationary signals. However, a similar falsification trial by Beck et al. (2006) produced consecutively false positives in all their six stationary cases.

This paragraph takes the occasion and offers future speculations on the usefulness of segments. If every changepoint is accepted as it is, segments can be defined in a series of μ_i since each CP indicates a border. After that, the distribution of spectrally homogenous segment lengths may be studied. In parallel, each segment can be described by an average DFT or PSD profile. Therefore, given a hypothetic database of many segments from several journeys, the segment length distribution joint with typical spectral shapes can lead to *spectral non-stationary* vibration simulations.

Subsection 4.1 gives an outlook on several other spectral descriptors, which may hopefully contribute to the measurement and analysis of SNS in RVV.

4.1 Further spectral descriptors

Spectral entropy, e, captures peaks (also called formants) of a spectrum (Misra et al., 2004), but each s_k spectrum shall be normalized, such as:

$$\tilde{s}_k = \frac{s_k}{\sum_{k=b_1}^{b_2} s_k}, \tag{14}$$

then the entropy can be calculated as:

$$e = -\sum_{k=b_1}^{b_2} \tilde{s}_k \log_2 \tilde{s}_k. \tag{15}$$

The ratio of the spectrum's geometric mean to its arithmetic mean is called spectral flatness (The MathWorks, Inc., 2021):

$$f_l = \frac{\left(\prod_{k=b_1}^{b_2} s_k\right)^{\frac{1}{b_2-b_1}}}{\frac{1}{b_2-b_1}\sum_{k=b_1}^{b_2} s_k}. \tag{16}$$

Noise shows a higher spectral flatness, while a lower spectral flatness reflects upon tonality.

The flatness measure in Eq. (16) has a plain shortcoming, namely $f_l = 0$ if any of $s_k = 0$. When s_k includes zero, the transition from flat to non-flat determination is not gradual. Madhu (2009) proposed an alternative:

$$\log_2(f_{l2}+1) = -\frac{1}{\log_2(b_2-b_1)}\sum_{k=b_1}^{b_2} \tilde{s}_k \log_2 \tilde{s}_k, \tag{17}$$

where s_k is normalized as of Eq. (14), yielding a scale-invariant, gradually increasing measure of flatness.

The ratio of the spectrum's peak to its arithmetic mean is called the spectral crest (The MathWorks, Inc., 2021):

$$c = \frac{\max\left(s_{k\epsilon[b_1,b_2]}\right)}{\frac{1}{b_2 - b_1}\sum_{k=b_1}^{b_2} s_k}, \tag{18}$$

reflect on the peakedness of the spectrum. More tonality suggests a higher spectral crest, while more noise yields a lower spectral crest.

Spectral flux is another measure of the spectrum's variability over time (ibid.):

$$f_x = \left(\sum_{k=b_1}^{b_2} \left|s_k(t) - s_k(t-1)\right|^p\right)^{\frac{1}{p}}, \tag{19}$$

with p denoting the type of norm. Spectral flux can be used for onset detection or audio segmentation.

The slope is related to the resonant properties of the vocal folds (ibid.):

$$s = \frac{\sum_{k=b_1}^{b_2}\left(f_k - \bar{f}_k\right)\left(s_k - \bar{s}_k\right)}{\sum_{k=b_1}^{b_2}\left(f_k - \bar{f}_k\right)^2}, \tag{20}$$

with $\bar{f}_k$ denoting the mean frequency and $\bar{s}_k$ denoting the mean spectral value. The spectral slope is more pronounced when the energy in the lower formants is greater than in the higher formants.

The spectral decrease, d, emphasizes the slopes of the lower frequencies (ibid.):

$$d = \frac{\sum_{k=b_1+1}^{b_2}\frac{s_k - s_{b_1}}{k-1}}{\sum_{k=b_1+1}^{b_2}s_k}. \tag{21}$$

Spectral slope and spectral decrease are often used in a complementary fashion.

The spectral roll-off point, r, determines the frequency bin, under which a κ proportion of the overall energy occurs and thereby calculates a bandwidth (ibid.):

$$r = i, \text{ such that } \sum_{k=b_1}^{i}\left|s_k\right| = \kappa\sum_{k=b_1}^{b_2}s_k. \tag{22}$$

with κ denoting an energy threshold (usually 85, 95%). The roll-off point is often implemented for audio scene analysis. Spectral descriptors $\{e, f_1, f_{l2}, c, f_x, s, d, r\}$ for measurement C are depicted in Fig. A1 in the Appendix.

5 Conclusion

The paper presented three experiments investigating the hypothesis of whether SNS exists in RVV. The RA tests showed confirmation of SNS corresponding to four spectral moments from STFT. Autocorrelation functions further discussed three cases of stationarity. The CPA found significant changepoints in the series of each investigated spectral descriptors of the measurements. Besides, an SNS metric was proposed for RVV analysis in the long term.

It was concluded that RVV undergoes changes in STFT thus changepoints are present in the spectral moments. Since PSD-based vibration simulations are stationary in time- and the frequency domain, the broad implication of current research leads to the need of spectral non-stationary simulations – whereby amplitude-type NS has been an active field of study in PVT. The findings supply a potential contribution to a mechanism for further non-stationary vibration simulations.

References

Beck, T. W., Housh, T. J., Weir, J. P., Cramer, J. T., Vardaxis, V., Johnson, G. O., Coburn, J. W., Malek, M. H., Mielke, M. (2006) "An Examination of the Runs Test, Reverse Arrangements Test, and Modified Reverse Arrangements Test for Assessing Surface EMG Signal Stationarity", Journal of Neuroscience Methods, 156(1–2), pp. 242–248.
https://doi.org/10.1016/j.jneumeth.2006.03.011

Bendat, J. S., Piersol, A. G. (2010) "Random Data: Analysis and Measurement Procedures", John Wiley & Sons, Inc. ISBN 9780470248775
https://doi.org/10.1002/9781118032428

Bilodeau, M., Cincera, M., Arsenault, A. B., Gravel, D. (1997) "Normality and Stationarity of EMG Signals of Elbow Flexor Muscles During Ramp and Step Isometric Contractions", Journal of Electromyography and Kinesiology, 7(2), pp. 87–96.
https://doi.org/10.1016/S1050-6411(96)00024-7

David, F. N., Siegel, S. (1957) "Review of Nonparametric Statistics for the Behavioral Sciences", Biometrika, 44(3/4), p. 538.
https://doi.org/10.2307/2332896

Dickey, D. A., Fuller, W. A. (1981) "Likelihood Ratio Statistics for Autoregressive Time Series with a Unit Root", Econometrica, 49(4), pp. 1057–1072.
https://doi.org/10.2307/1912517

Faber, M. H. (2012) "Statistics and Probability Theory: In Pursuit of Engineering Decision Support", Springer. ISBN 978-94-007-4055-6
https://doi.org/10.1007/978-94-007-4056-3

Gagniuc, P. A. (2017) "Markov Chains: From Theory to Implementation and Experimentation", John Wiley & Sons, Inc. ISBN 9781119387558
https://doi.org/10.1002/9781119387596

Grey, J. M., Gordon, J. W. (1978) "Perceptual effects of spectral modifications on musical timbres", The Journal of the Acoustical Society of America, 63(5), pp. 1493–1500.
https://doi.org/10.1121/1.381843

Hári, L. R., Földesi, P. (2022) "Evaluation of a CUSUM-Type Changepoint Detector Applied in the Time-Frequency Domain of Synthetic Road Vehicle Vibrations", In: Vehicle and Automotive Engineering 4, Miskolc, Hungary, pp. 812–823. ISBN 978-3-031-15210-8
https://doi.org/10.1007/978-3-031-15211-5_67

Jongman, A., Wayland, R., Wong, S. (2000) "Acoustic characteristics of English fricatives", The Journal of the Acoustical Society of America, 108(3), pp. 1252–1263.
https://doi.org/10.1121/1.1288413

Kowalewski, M., Novack-Gottshall, P. (2010) "Resampling Methods in Paleontology", The Paleontological Society Papers, 16, pp. 19–54.
https://doi.org/10.1017/S1089332600001807

Kwiatkowski, D., Phillips, P. C. B., Schmidt, P., Shin, Y. (1992) "Testing the null hypothesis of stationarity against the alternative of a unit root: How sure are we that economic time series have a unit root?", Journal of Econometrics, 54(1–3), pp. 159–178.
https://doi.org/10.1016/0304-4076(92)90104-Y

Leybourne, S. J., HcCabe, B. P. M. (1999) "Modified Stationarity Tests with Data-Dependent Model-Selection Rules", Journal of Business & Economic Statistics, 17(2), pp. 264–270.
https://doi.org/10.1080/07350015.1999.10524816

Lo, A.W., MacKinlay, A. C. (1988) "Stock Market Prices Do Not Follow Random Walks: Evidence from a Simple Specification Test", Review of Financial Studies, 1(1), pp. 41–66.
https://doi.org/10.1093/rfs/1.1.41

Madhu, N. (2009) "Note on Measures for Spectral Flatness", Electronics Letters, 45(23), pp. 1195–1196.
https://doi.org/10.1049/el.2009.1977

Misra, H., Ikbal, S., Bourlard, H., Hermansky, H. (2004) "Spectral Entropy Based Feature for Robust ASR", In: 2004 IEEE International Conference on Acoustics, Speech, and Signal Processing, Montreal, QC, Canada, pp. I–193. ISBN 0-7803-8484-9
https://doi.org/10.1109/ICASSP.2004.1325955

Page, E. S. (1954) "Continuous Inspection Schemes", Biometrika, 41(1/2), pp. 100–115.
https://doi.org/10.2307/2333009

Page, E. S. (1955) "A Test for a Change in a Parameter Occurring at an Unknown Point", Biometrika, 42(3/4), pp. 523–527.
https://doi.org/10.2307/2333401

Page, E. S. (1957) "On problems in which a change in a parameter occurs at an unknown point", Biometrika, 44(1–2), pp. 248–252.
https://doi.org/10.1093/biomet/44.1-2.248

Phillips, P. C. B., Perron, P. (1988) "Testing for a unit root in time series regression", Biometrika, 75(2), pp. 335–346.
https://doi.org/10.1093/biomet/75.2.335

Pradhan, R. P. (2012) "Variance Ratio Test of Random Walk for Foreign Trade: The Study in India During the Globalization Era of 1990s", International Journal of Financial Research, 3(1), pp. 101–104.
https://doi.org/10.5430/ijfr.v3n1p101

Rouillard, V. (2014) "Quantifying the Non-stationarity of Vehicle Vibrations with the Run Test", Packaging Technology and Science, 27(3), pp. 203–219.
https://doi.org/10.1002/pts.2024

Shewhart, W. A., Deming, W. E. (1986) "Statistical Method from the Viewpoint of Quality Control", Dover Publications. ISBN 9780486652320

Taylor, W. A. (2000) "Change-Point Analysis: A Powerful New Tool for Detecting Changes", [pdf] Taylor Enterprises, Inc., Baxter Healthcare Corporation, Round Lake, IL, USA, Available at: https://variation.com/wp-content/uploads/change-point-analyzer/change-point-analysis-a-powerful-new-tool-for-detecting-changes.pdf [Accessed: 15 April 2021]

The MathWorks, Inc., (2021) "Audio ToolboxTM Reference Guide: Matlab & Simulink", [pdf] The MathWorks, Inc., Natick, MA, USA. Available at: https://www.mathworks.com/help/pdf_doc/audio/audio_ref.pdf [Accessed: 15 April 2021]

US Army Test and Evaluation Command (2019) "MIL-STD-810H Test Method Standard: Environmental Engineering Considerations and Laboratory Tests", The US Department of Defense, Aberdeen Proving Ground, Maryland, USA.

Appendix

Measurement C: STFT and other spectral descriptors
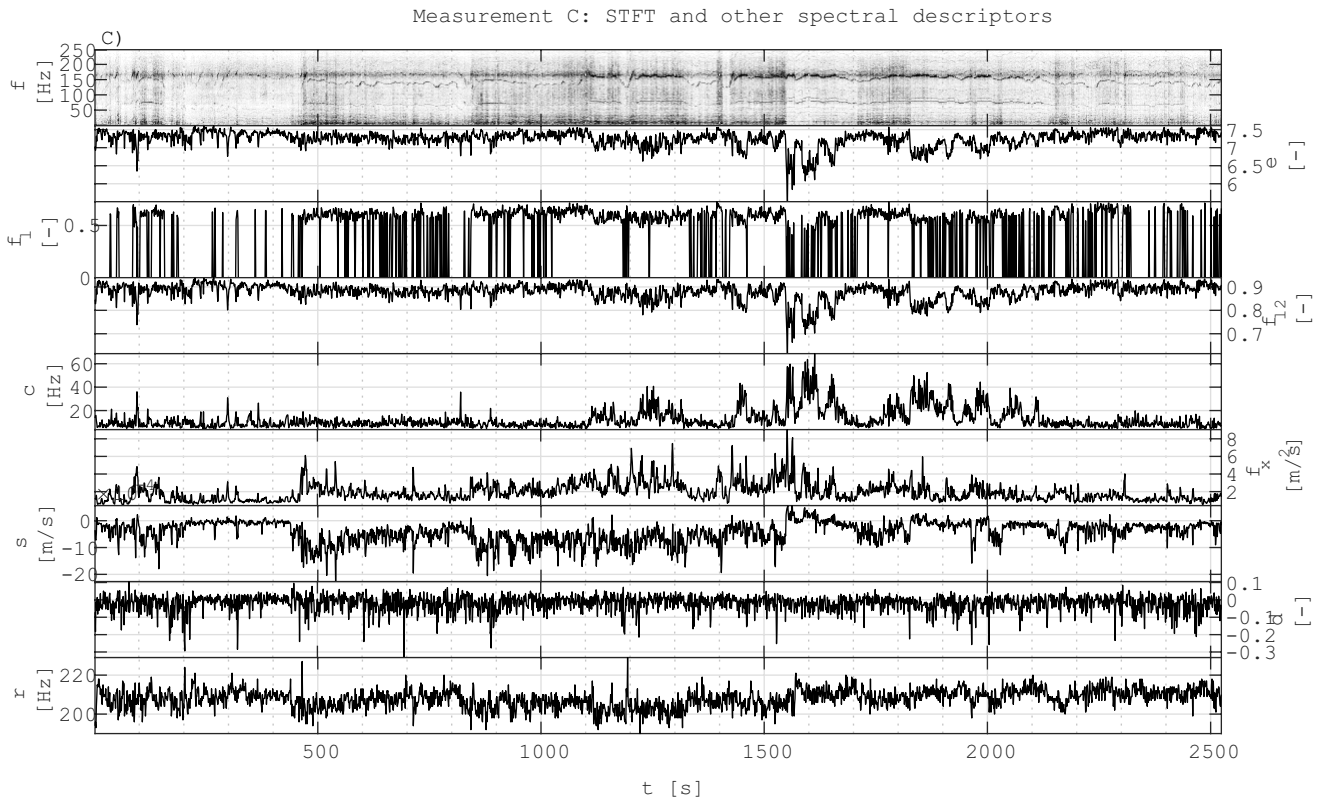
Fig. A1 Short-time Fourier transform of measurement *C*, beneath spectral descriptors as noted by axis labels: *e* spectral entropy, f_l spectral flatness (Eq. (16)), f_{l2} modified spectral flatness (Eq. (17)), *c* spectral crest, f_x spectral flux at $p = 2$ norm, *s* spectral slope, *d* spectral decrease, *r* roll-off point at $\kappa = 0.95$